Biochimica et Biophysica Acta, 1142 (1993) 240–252

BBABIO 43811

X-ray absorption spectroscopy of oriented cytochrome oxidase

Graham N. George [a,1], Stephen P. Cramer [b], Terrence G. Frey [c] and Roger C. Prince [a]

[a] *Exxon Research and Engineering Co., Annandale, NJ (USA),* [b] *Department of Applied Science, University of California, Davis, CA (USA) and* [c] *Department of Biology, San Diego State University, San Diego, CA (USA)*

(Received 23 November 1992)

Key words: Cytochrome oxidase; Membranous multilayer; X-ray absorption spectroscopy; EXAFS

The polarized X-ray absorption spectra of the copper, iron and zinc sites of mitochondrial cytochrome oxidase in oriented membrane multilayers have been examined. The copper X-ray absorption edge spectra indicate the presence of a tetragonal copper, which we assign as Cu_B, oriented with the long axis approximately orthogonal to the membrane normal. We have also detected the presence of a relatively long (2.6 Å) Cu–S or Cu–Cl interaction, which we assign to a copper-thioether (probably Met_{210}) coordination at the Cu_A site, with the bond oriented along the membrane normal. The coordination of the zinc, the iron and the Cu_B heme a_3 binuclear site are discussed.

Introduction

Mammalian cytochrome oxidase is the terminal electron carrier in mitochondrial respiration, accepting electrons from ferrocytochrome *c* and reducing oxygen to water in a four electron process. It contains two hemes, *a* and a_3, two copper atoms, Cu_A and Cu_B, and a single zinc. Heme a_3 and Cu_B form an antiferromagnetically coupled binuclear site which is thought to be the site of oxygen reduction, while heme *a* and Cu_A appear to be more electronically independent [1–3], and apparently serve to deliver electrons to the heme a_3–Cu_B binuclear site (see Ref. 1 for a recent review). The function of the zinc is unknown. To date, there is little structural information available from X-ray crystallography [4] and most of our knowledge of the active site structures has come from other techniques, and in particular spectroscopy and genetic studies. A number of different spectroscopic techniques have been applied in attempts to characterize the structure of the electron transfer chromophores. These techniques can yield additional angular information if applied to oriented or partially oriented samples such as oriented membrane multilayers. Thus, the orientation of the heme planes has been determined by polarized electronic absorption and EPR spectroscopy; the heme normals being perpendicular to the membrane normal [5–9] and the angle between the Fe-Fe vector and the heme normal being 30–60° [10].

Information about the atomic neighborhood of the metal sites can be obtained from X-ray absorption fine structure (XAFS) spectroscopy, but there has been considerable controversy about the XAFS of cytochrome oxidase [11–17]. While the experimental data from the two principal protagonists may [16,17], or may not [11], be similar, the structural conclusions have been the focus of debate for some years. We have taken advantage of the highly plane polarized nature of synchrotron radiation to study cytochrome oxidase in oriented mitochondrial membrane multilayers.

Materials and Methods

Sample preparation and characterization

Membranous cytochrome *c* oxidase was prepared as previously described [18] and oriented by partial dehydration [5] supported on a mylar substrate. The resulting films of membranous cytochrome oxidase were approximately 0.1 mm thick, we estimate an approximate enzyme concentration of 5–10 mM. The EPR spectra of the untreated oriented samples indicated a similar intrinsic disorder, or mosaic spread, to the preparations of others [9]. EPR spectroscopy of the fluoride complexed form indicated that the oxidase in our preparations was the form of the resting enzyme called 'oxygenated' [19]. Naqui et al. [20], and later Baker et al. [21], showed that CN^- binding kinetics can be used as a sensitive indicator of active site integrity.

Correspondence to: G.N. George at [1] Present address: Stanford Synchrotron Radiation Laboratory, Stanford University, SLAC, P.O. Box 4349, Bin 69, Stanford, CA 94309, USA.

Multiple binding rates are commonly observed with most isolated preparations, and the most rapidly reacting form is considered to be the least adulterated [20–22]. In agreement with Baker et al. [21], the CN^- binding kinetics of our membranous preparations indicated that more than 90% of our enzyme was in the 'fast' binding form prior to partial dehydration.

Data collection

Electron paramagnetic resonance (EPR) spectra were recorded on a Varian E-109 instrument equipped with an Oxford instruments liquid helium flow cryostat and an EIP 548A microwave frequency counter, interfaced to an ACT Apricot Xi computer. Spectra were transferred to a Digital Equipment Corporation VAX 11-8530 computer for manipulation.

X-ray absorption spectroscopy was conducted at the Stanford Synchrotron Radiation Laboratory, with the electron storage ring SPEAR operating in dedicated mode (3.0 GeV, 30–70 mA). X-ray absorption was measured by monitoring the fluorescence excitation spectrum using either a fluorescent ion chamber detector with suitable filters and slit assembly [23,24], or an array of intrinsic germanium detectors [25]. The edge spectra were recorded on beam lines IV-2 and VII-3 using Si(220) double crystal monochromators. The iron EXAFS (extended X-ray absorption fine structure) spectra were recorded on beam lines IV-2 and VI-2 with focussing and using Si(111) and Ge(111) monochromators, respectively. Beam line IV-2 (focused) with Si(111) monochromator crystals was used for the acquisition of the copper and zinc EXAFS spectra. EXAFS spectra were typically averages of four to eight 20 min scans. During data collection the samples were held at a temperature close to 4 K in an Oxford instruments CF1204 liquid helium flow cryostat. Even at these low temperatures, samples showed gradual deterioration (as detected by changes in the Cu K-edge spectra), possibly photoreduction by hydrated electrons liberated by the incident radiation. Exposure of individual samples was therefore minimized, with samples being kept in the beam for no more than 12 h.

Data analysis

The experiments were conducted by rotating the membranous multilayer sample and measuring the EXAFS spectra as a function of the angle between the X-ray **e**-vector and the membrane normal. The EXAFS spectra, $\chi(k)$, of the individual orientations were quantitatively analyzed by curve fitting to the approximate expression:

$$\chi(k) = \sum_{b=1}^{n} \frac{N_b F_{ab}(\theta) A_{ab}(k,R_{ab})}{kR_{ab}^2} \exp\left(\frac{-2R_{ab}}{\lambda_{ab}(k,R_{ab}))}\right) \times \exp(-2\sigma_{ab}{}^2 k_{ab}{}^2) \sin[2kR_{ab} + \alpha_{ab}(k,R_{ab})]) \quad (1)$$

In which $A_{ab}(k,R_{ab})$ and $\alpha_{ab}(k,R_{ab})$ are the EXAFS total amplitude and phase-shift functions, respectively, k is the photoelectron wave number, N_b the number of b-type atoms at a mean distance R_{ab} from the absorber atom a, λ_{ab} the photo-electron mean free path and σ the root mean square deviation of R_{ab}. The angular dependence of the EXAFS amplitude is approximated by including the function $F_{ab}(\theta)$. The functions $A_{ab}(k,R_{ab})$ and $\alpha_{ab}(k,R_{ab})$ were calculated by using the program feff of Rehr and co-workers [26,27], except for outer shell heme carbon atoms which were extracted from the EXAFS of iron tetraphenyl porphyrin chloride. For K-edge EXAFS, the angular variation in EXAFS amplitude is, to a first approximation, simply equal to 3 $\cos^2\beta$, where β is the angle between the X-ray electric field vector (**e**) and the absorber-backscatterer (a-b) vector [28], and assuming an unoriented (polycrystalline) EXAFS amplitude of unity. It should be noted that for the sake of simplicity we have neglected the curved wave terms in the EXAFS orienta-

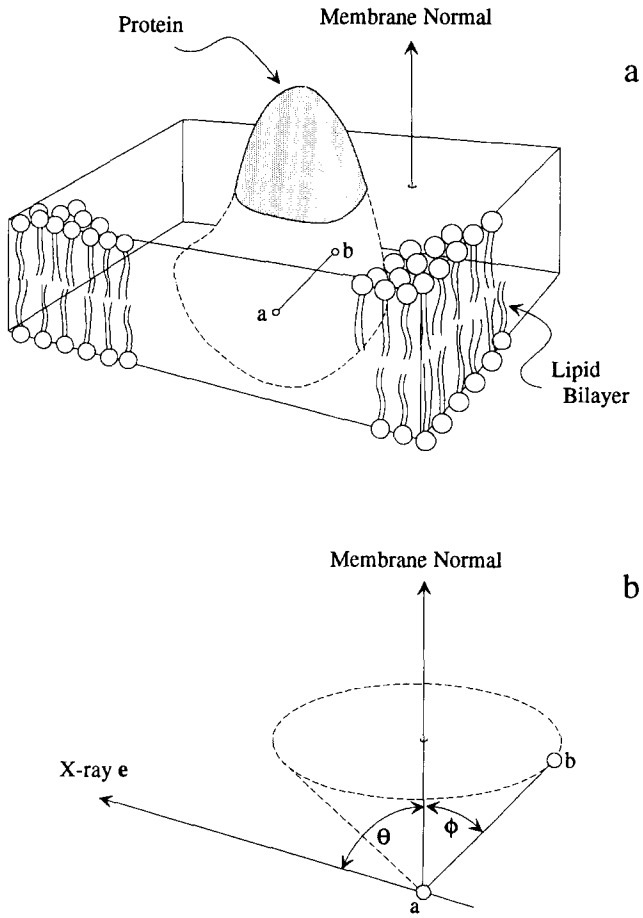

Fig. 1. The coordinate system used for XAFS spectroscopy of oriented membranous multilayers. The upper diagram shows a schematic view of a lipid bilayer, together with an intrisic protein containing an absorber-backscatterer pair (denoted by a and b). The lower diagram shows details of the coordinate system, defining the symbols used in the text. The dashed line shows the rotational symmetry of the membranous multilayer samples.

tion dependence. These will be maximal at low k-values and are expected to be quite small, having additional terms in $\sin^2\beta$ (Ref. 28 and references therein) and result in orientation-dependent phase and amplitude functions. Approximating the effects of sample disorder by a Gaussian distribution in orientations, $F_{ab}(\theta)$, is given by Eqn. 2 (George et al., Refs. 29,30).

$$F_{ab}(\theta) = \frac{1}{2}\left\{\int_0^{\pi}(\sin^2\theta\sin^2\phi + 2\cos^2\theta\cos^2\phi) \times \sin\phi\exp\left[-\ln 2(\phi-\phi_{ab})^2/\Omega^2\right]d\phi\right)\Bigg\} \times\left\{\int_0^{\pi}\sin\phi\exp\left[-\ln 2(\phi-\phi_{ab})^2/\Omega^2\right]d\phi\right\}^{-1} \quad (2)$$

in which θ is the experimentally varied angle between the membrane normal and the X-ray e-vector, ϕ_{ab} is the angle between the a-b vector and the membrane normal (see Fig. 1), and Ω is the half-width of the Gaussian distribution of ϕ_{ab}.

The angular variation of dipole-allowed bound state transitions will also be described by Eqn. 2, except that in this case ϕ_{ab} is the angle between the membrane normal and the transition dipole operator. As dipole-allowed transitions are expected to be to orbitals of mostly p-character, then ϕ_{ab} will be simply the angle between the axis of the p-orbital and the membrane normal.

For sites with EXAFS from more than one scatterer of a given type, at distances differing by less than the EXAFS resolution, it is not possible to obtain the values of the individual ϕ_{ab}s. Nevertheless, an average value $\langle\phi\rangle$ can be obtained, defined by Eqn. 3, in which n_b is the number of indistinguishable a–b interactions.

$$\cos\langle\phi\rangle = \sqrt{\frac{\sum_{b=1}^{n_b} n_b\cos^2\phi_{ab}}{\sum_{b=1}^{n_b} n_b}} \quad (3)$$

EXAFS data were analyzed by first fitting individual EXAFS spectra, measured at different values of θ, to Eqn. 1 to obtain values of R_{ab}, σ_{ab}, and an amplitude $F_{ab}(\theta).N_b$ for each scatterer b. Values for apparent coordination number, N_b, and average relative orientation, $\langle\phi\rangle$, were then obtained by fitting the θ dependence of the amplitude, i.e., $[F_{ab}(\theta)N_b]$ using Eqn. 2, which was solved numerically, using values for Ω (in most cases $\Omega \cong 17°$) obtained by simulation of the EPR spectra of heme a and Cu_A.

Results

The X-ray fluorescence excitation spectrum of a typical sample of cytochrome c oxidase is shown in Fig. 2a; the iron, copper and zinc K-edges are at about 7110 eV, 8980 eV and 9660 eV, respectively, and the corresponding EXAFS are clearly visible as small oscillations on the high-energy side of each edge. The X-ray fluorescence emission spectrum of a similar sample is shown in Fig. 2b, which was measured with the energy dispersive detector. It shows the K_α and K_β fluorescence lines of all three metals. It is important to note that the amplitude of the iron K edge (and to a much

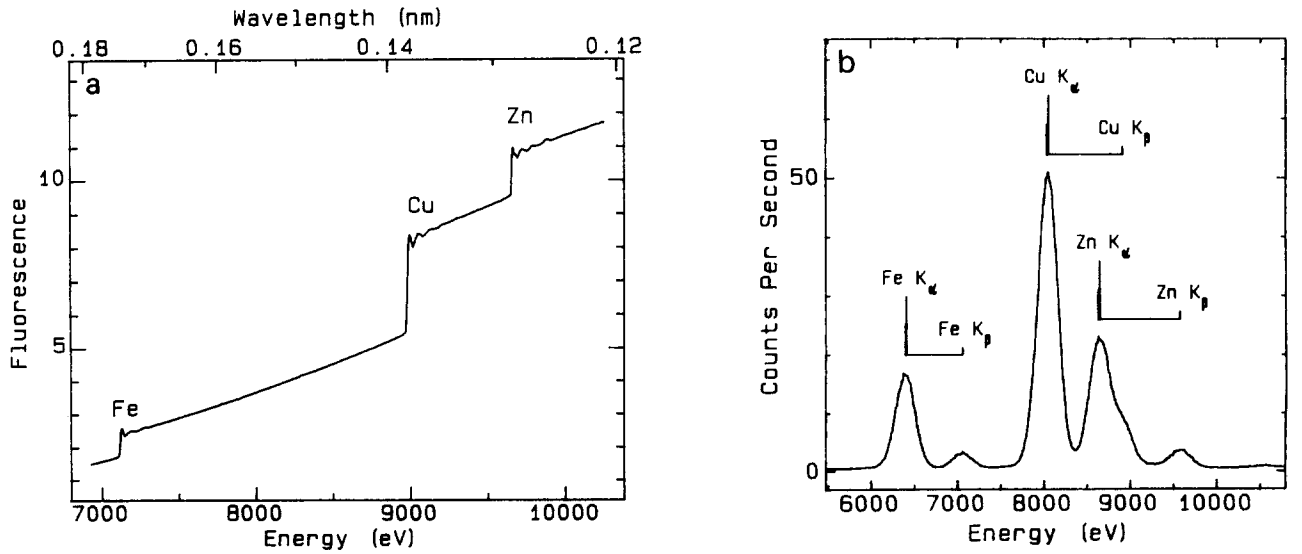

Fig. 2. X-ray fluorescence excitation (a) and emission spectra (b) of membranous cytochrome oxidase. In (a) the total X-ray fluorescence was recorded (i.e., the detector was opetated in a non-dispersive mode); the iron, copper and zinc X-ray absorption K-edges are clearly visible. In (b) the energy dispersive output of a single element of the 13 element Ge detector array (see Materials and Methods) is shown; the copper, iron and zinc fluorescence lines can be clearly seen.

lesser extent the copper edge) is artifactually reduced, relative to the zinc edge, because of significantly greater attenuation of the iron X-ray fluorescence by the sample, the cryostat windows and the atmosphere separating the sample and the detector. Thus, the relative edge jumps are not directly proportional to the relative metal contents. Using the tabulated X-ray cross sections of McMaster et al. [31] and correcting for fluorescence yield and experimental attenuation of the fluorescence, we calculate relative metal contents (assuming two irons per subunit) of 2.0 Fe/1.8 Cu/0.8 Zn (i.e., 2:2:1). Similar relative values were also obtained by comparing the edge jumps of the transmittance spectra (not illustrated). While these values agree with conventional wisdom (cf. Ref. 32), they differ with recent work [4,33,34] which suggests the presence of additional copper, sometimes called Cu_C.

Copper K-edge spectra

Fig. 3a shows the orientation dependence of the membranous cytochrome oxidase copper K absorption edge. Several features show a marked angular dependence. The most noticeable are the peak at 8987 eV, which is most intense at $\theta = 90°$, and the broad feature close to 9003 eV, which is most intense at $\theta = 14°$. The smaller feature at 8993 eV, which is most apparent in the second derivative spectra, is most pronounced at $\theta = 90°$. Other features, such as those near 8983 eV and 8997 eV, show less well defined dichroism.

In terms of X-ray absorption edge spectra, copper (II) is probably the most intensively investigated of all of the transition ions, and considerable model compound data, including single crystal studies, are available in the literature [35–38]. Cu(II) complexes of tetragonal geometry have quite characteristic edge spectra, for which three major, highly polarized, absorptions have been assigned [36–38]. Two of these features, at about 8987 eV and 8993 eV, are most intense when **e** is parallel to the z-axis; they have been assigned as $1s \rightarrow 4p_z$ + shake-down and a combination of $1s \rightarrow 4p_z$ and $1s \rightarrow 5p_z$ + shake-down, respectively [36,38]. The third major feature manifests itself as a rather broad absorption close to 9000 eV, most intense when **e** is perpendicular to z. The latter absorption is supposed to be due mainly to $1s \rightarrow 4p\sigma$, together with $1s \rightarrow 5p\sigma$ transitions [36,38].

The 8987 eV, 8993 eV and 9003 eV features of the cytochrome oxidase Cu K edge spectra are characteristic of tetragonal Cu(II), and we conclude that one of the two coppers in cytochrome oxidase possesses this geometry. EPR spectroscopy of Cu_A clearly eliminates this site as a candidate, for although the spectra are not properly understood, they cannot arise from tetragonal Cu(II) (see Ref. 39 and references therein). We therefore conclude that Cu_B of resting cytochrome oxidase is tetragonal. The orientation dependence of intensity for a $1s \rightarrow 4p_z$ + shake-down transition is expected to be adequately described by Eqn. 2 and a least-squares fit of Eqn. 2 to the cytochrome oxidase Cu K edge 8987 eV peak is shown in Fig. 3b. The fit indicates that the tetragonal copper is oriented similarly to the hemes [6–9] with respect to the membrane

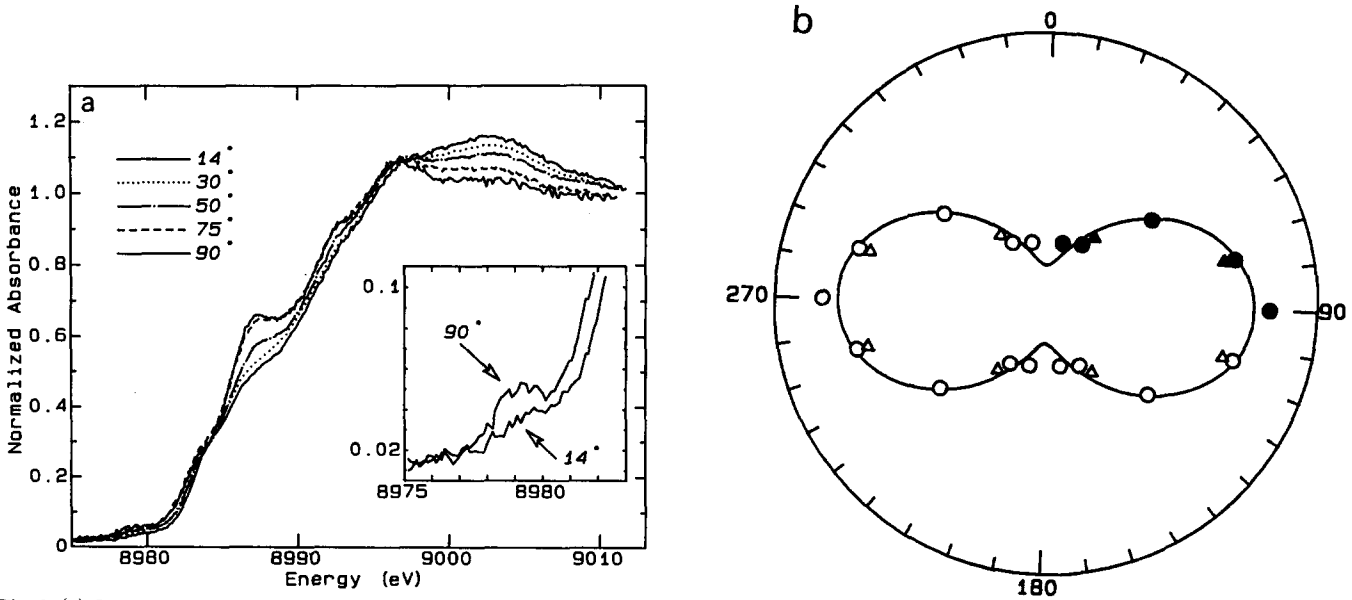

Fig. 3. (a) Copper K-edge spectra of oriented cytochrome oxidase for various membrane orientations with respect to the X-ray e-vector. The inset shows the orientation dependence of the $1s \rightarrow 3d$ feature. (b) Orientation dependence of the amplitude (measured as the amplitude of the second derivative of the absorption spectrum) of the 'shake-down' feature close to 8987 eV. The data points plotted as filled symbols show actual experimental points and those plotted as open symbols are the experimental data mirrored for clarity; the solid line shows the best fit to Eqn. 2.

normal; the z-axis being essentially perpendicular (83 $\pm$ 10°) to the membrane normal. For a square planar geometry, which is by far the most common among tetragonal Cu(II) complexes, the plane would be oriented perpendicular to the membrane plane.

A distinct $1s \rightarrow 3d$ transition at 8979 eV can also be seen in Fig. 3, and a close examination of the data indicate that this also possesses some angular dependence (see the inset on Fig. 3), being most intense at $\theta = 90°$. $1s \rightarrow 3d$ transitions are formally dipole forbidden but gain intensity either from a mixing of p-type orbitals, or by virtue of the fact that the quadrupole transition moment is, although small, significant [28,35]. If the $3d$ orbital has little mixing with p-orbitals (e.g., in a centrosymmetric complex), then rather weak transitions, with complicated angular dependency (not described by Eqn. 2), are expected [28]. For low symmetry sites, such as Cu_A, considerable $3d$-p mixing seems likely, and it seems probable that a large contribution to the $1s \rightarrow 3d$ transition may come from Cu_A. Although Cu_A is spectroscopically unique in many respects, the copper sites which it most resembles are the type 1 copper proteins. These proteins generally contain copper coordinated to two histidine nitrogens and one cysteine sulfur, which form a strong equatorial ligand field, plus a more distant axial coordination which, in plastocyanin (a typical type 1 copper protein), is methionine sulfur. The single crystal copper X-ray absorption spectra of plastocyanin have been studied in detail by Penner-Hahn et al. [40]. The Cu K-edge spectra show quite intense $1s \rightarrow 3d$ transitions, which are strongest when **e** is pointed in the equatorial plane [40]. If Cu_A does possess coordination resembling the type 1 copper site of plastocyanin, then the dichroism of the $1s \rightarrow 3d$ transition suggests that the Cu_A equatorial plane is oriented parallel to the membrane plane.

Copper EXAFS Fourier transforms and EXAFS curve fitting

Resting cytochrome oxidase The Fourier transforms of the copper EXAFS spectra at four different orientations are shown in Fig. 4, and the corresponding EXAFS spectra in Fig. 5a. All the Fourier transforms display two first-shell peaks with maxima close to R $\cong$ 1.9 Å and 2.3 Å. Because EXAFS cannot distinguish between scattering atoms of similar atomic number, there is always a certain ambiguity about the exact nature of the detected scatterers. Thus, while sulfur and nitrogen are quite easy to tell apart ($\alpha(k)$ and $A(k)$ are quite different), sulfur and chlorine scatterers yield essentially indistinguishable EXAFS. The 1.9 Å and 2.3 Å Fourier transform peaks can be attributed to Cu-(N,O) (i.e., Cu-N or Cu-O) and to Cu-(S,Cl) EXAFS, respectively. Angular dependent changes in both Cu-(N,O) and Cu-(S,Cl) peaks in the transforms shown in Fig. 4 are clearly apparent. Curve fitting of the

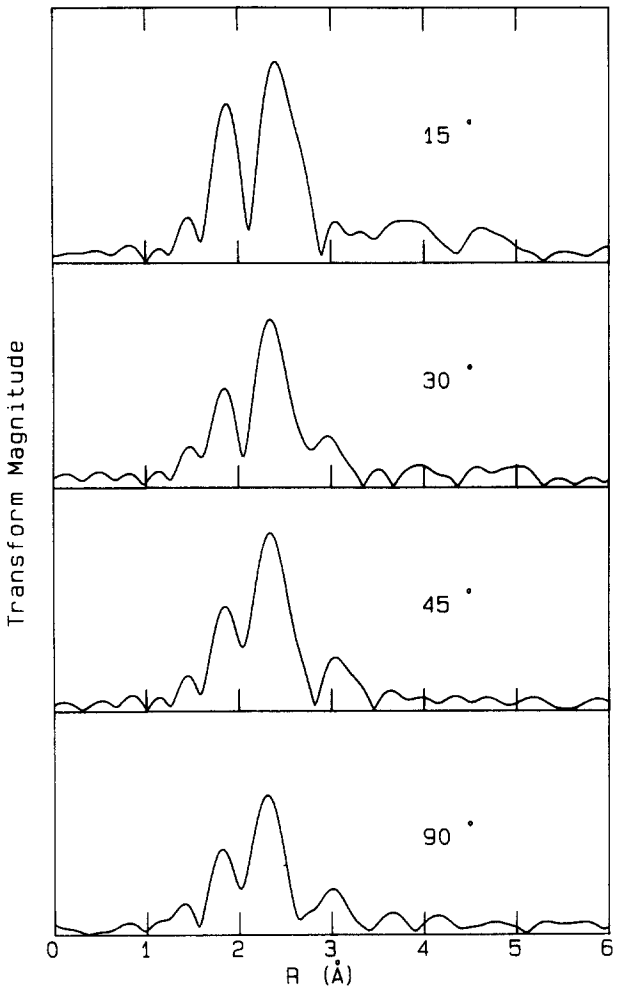

Fig. 4. (a) Copper K-edge EXAFS Fourier transforms of oriented cytochrome oxidase. The transforms have been phase-corrected for Cu-S.

EXAFS data (Fig. 5a, Table I) indicate that the data can be fitted with a minimum of three components – a Cu-(N,O) shell at 1.97 Å, Cu-(S,Cl) at 2.3 Å and a Cu–(S,Cl) interaction at 2.6 Å. The latter interaction becomes progressively more evident in the data as $\theta \rightarrow 0°$, and is a major component of the EXAFS at the smallest θ (14°). Fig. 5b shows polar plots of the amplitudes of the three interactions, together with least squares fits to Eqn. 2. These fits yield approximate coordination numbers and average orientations $\langle\phi\rangle$ for each shell of scatterers. The 1.97 Å Cu-(O,N) EXAFS corresponds to 1–2 interactions (per two coppers) at $\langle\phi\rangle = 37°$, the 2.3 Å Cu-(S,Cl) to 2–3 interactions at $\langle\phi\rangle = 46°$ and the 2.6 Å Cu-(S,Cl) to 0.5–1 interactions at $\langle\phi\rangle = 0°$ (Table I). The apparent bond length for the Cu–(O,N) and 2.3 Å Cu–(S,Cl) interactions varies slightly with ϕ (1.976–1.962 Å and 2.302–2.314 Å, respectively, see Table I). Although these changes are less than the EXAFS accuracy of $\pm$0.02 Å, they are probably significant, as errors arise primarily from non-transferrability of the phase functions

$\alpha_{ab}(k)$, and for similar interactions a relative precision of better than 0.01 Å is expected. The explanation for the apparent variation in bond length lies with the fact that the observed EXAFS represent averages of similar interactions each with distinct ϕ_{ab} and R_{ab} values (the latter differing by less than the EXAFS resolution of 0.12 Å). Thus, for θ values where the EXAFS from shorter bonds (for example) predominates (Eqn. 2) the measured (average) bond length will be shorter. The θ dependence of the determined R_{ab} values therefore represents the angular distribution of the individual bond lengths at the active sites.

While the Cu–(N,O) and the 2.3 Å Cu–(S,Cl) interactions have been detected in previous EXAFS studies of (non-oriented) cytochrome oxidase, the 2.6 Å Cu–(S,Cl) was not detected in earlier work. The most probable reason for this is that the contribution of the long Cu–(S,Cl) to the EXAFS of polycrystalline samples is rather small and therefore easily missed. For oriented samples, however, when $\theta \rightarrow 0°$, there is an

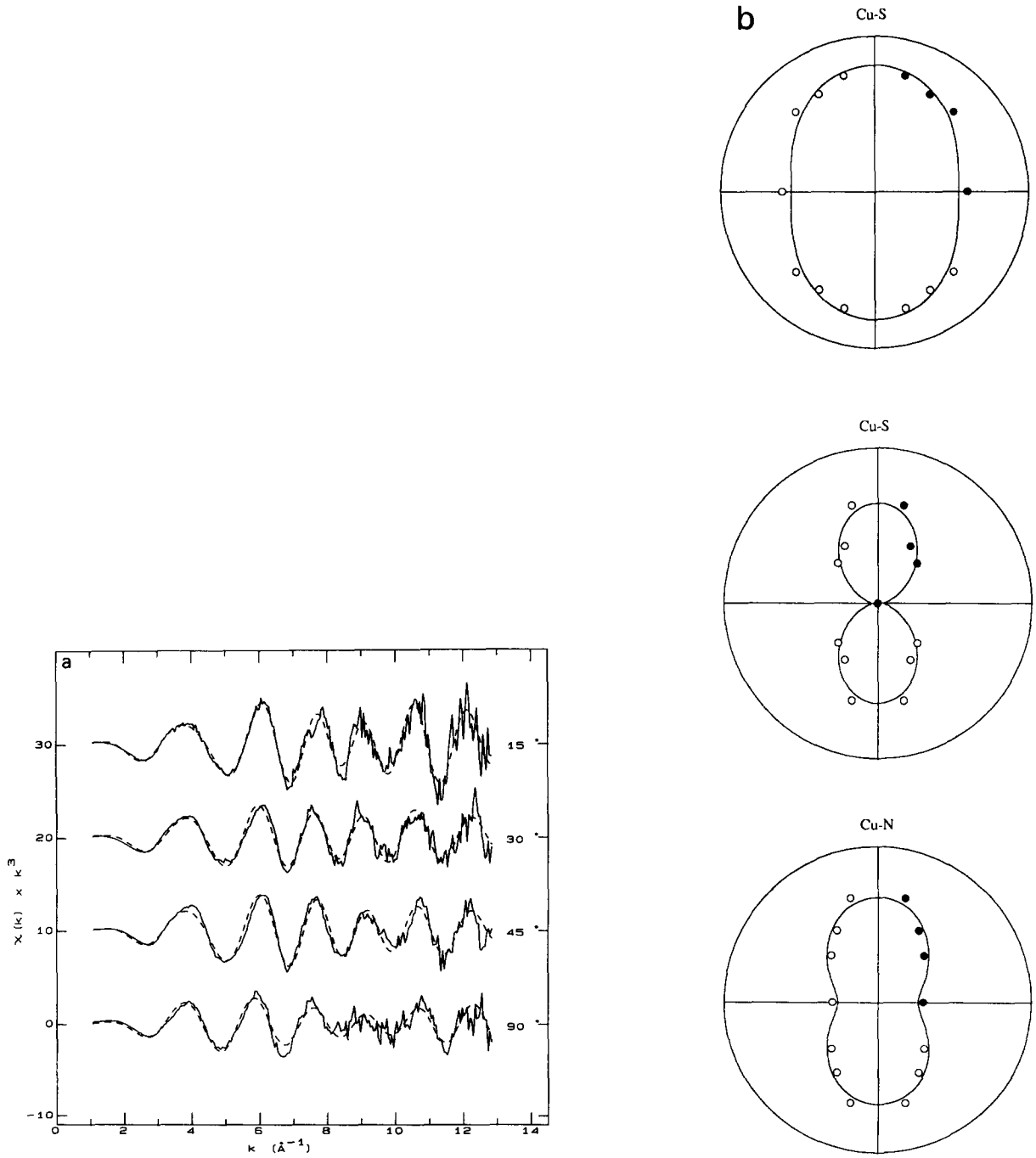

Fig. 5. (a) Copper EXAFS spectra (solid lines) and best fits (broken lines) using the parameters given in Table I. (b) Polar plots of orientation dependence of the amplitudes of the 1.97 Å Cu–(O,N), the 2.3 Å Cu–(S,Cl) and the 2.6 Å Cu–(S,Cl) interactions.

TABLE I

Curve-fitting parameters for cytochrome oxidase oriented membranous multilayer copper EXAFS

The values for σ^2 were fixed at the chemically reasonable value of 0.0021 Å^2 and 0.0035 Å^2, for the resting and cyanide inhibited enzyme, respectively, which were also the all-round best-fit values. The quantity $F(\theta)\ N$ is the product of the coordination number, N, and the angular dependence of EXAFS amplitude as defined in Eqns. 1, 2 and 3 in the Materials and Methods section. Note that the values for N are not normalized to the metal content of the enzyme.

	Resting enzyme					
	Cu–N		Cu–S		Cu–S	
θ	$F(\theta)\ N$	R (Å)	$F(\theta)\ N$	R (Å)	$F(\theta)\ N$	R (Å)
15°	2.406	1.951	1.165	2.281	1.392	2.613
30°	1.577	1.944	1.255	2.276	0.848	2.640
45°	1.662	1.954	1.293	2.261	0.757	2.616
90°	1.288	1.961	1.154	2.276	0.007	2.616
	Cyanide-Inhibited Enzyme					
	Cu–N		Cu–S		Cu–S	
θ	$F(\theta)\ N$	R (Å)	$F(\theta)\ N$	R (Å)	$F(\theta)\ N$	R (Å)
15°	2.402	1.926	1.814	2.265	1.371	2.619
90°	2.186	1.937	2.010	2.258	0.0	-

approximately 3-fold enhancement of the amplitude relative to the polycrystalline EXAFS, and its presence then becomes quite evident. In agreement with this, the fit of the Cu EXAFS of polycrystalline cytochrome oxidase (an unoriented suspension of the membrane vesicles, not illustrated) was improved subtly but significantly by addition of one long sulfur (per two coppers) at 2.6 Å and, subsequent to our preliminary report [41], this has been confirmed by others [42].

Cyanide-inhibited cytochrome oxidase

Cyanide is known to specifically disrupt the Cu_B-heme a_3 site (Ref. 32 and Refs. therein), possibly by forming a bridge between the metals (e.g., Cu-NC-Fe) although CN^- may bind to Cu_B and heme a_3 separately [43]. In an attempt to resolve the individual contributions of Cu_A and Cu_B we chose to study the copper K-edge EXAFS of the cyanide-inhibited enzyme. The EXAFS Fourier transforms of two different orientations, $\theta = 15°$ and $\theta = 90°$, are shown in Fig. 6a and the EXAFS plus curve-fitting results in Fig. 6b. The spectra are markedly different from those reported earlier by Cramer and co-workers [44], which showed little or no Cu-S EXAFS and intense outer-shell EXAFS. It seems probable from the unusual nature of the spectra and the harsh experimental conditions used in the earlier work, that the cyanide treatment of Scott et al. [44] extracted the copper from the enzyme, yielding the $Cu(CN)_4^{3-}$ anion or higher homologs. In contrast, the data reported here are quite similar to those from the resting enzyme, but with significant differences. The curve-fitting analysis clearly shows that the 2.6 Å Cu interaction observed in the resting enzyme (see above) is still present in the cyanide-inhibited form, indicating that it does not come from a bridge between Cu_B and heme a_3.

Iron K-edge spectra

The iron K-edge spectra for two different sample orientations are shown in Fig. 7. Significant anisotropy

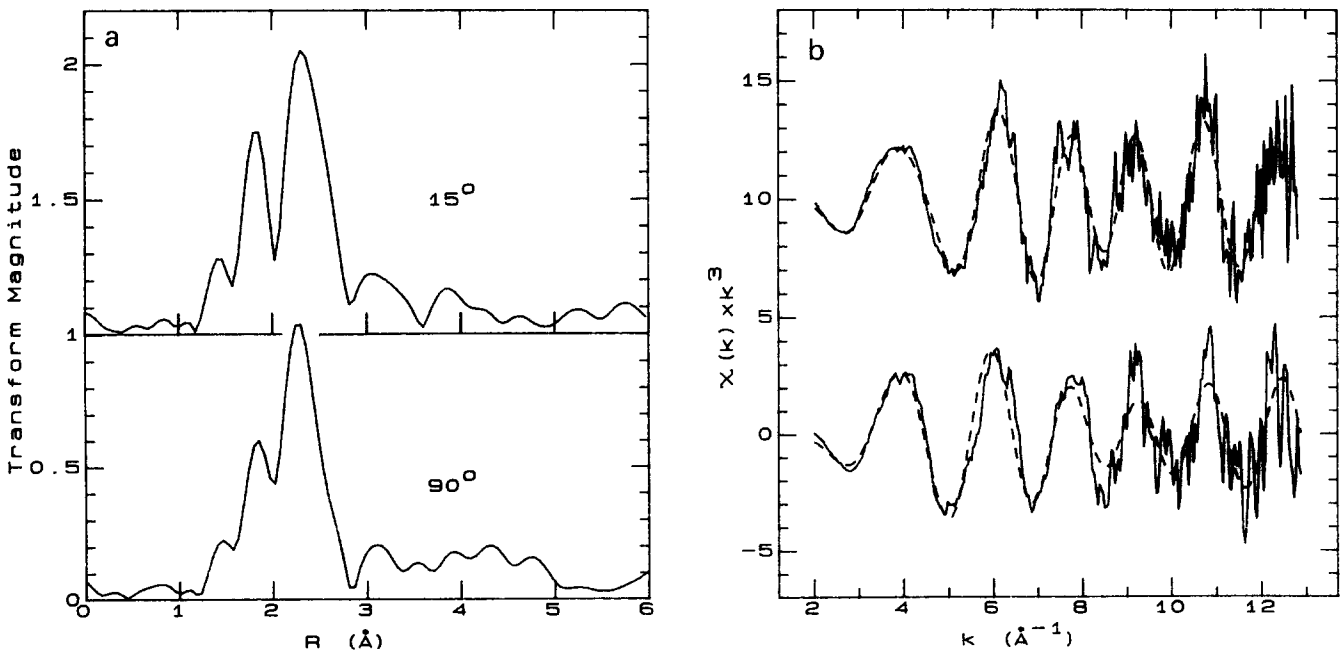

Fig. 6. (a) Copper K-edge EXAFS Fourier transforms of cyanide inhibited oriented cytochrome oxidase and (b) shows the corresponding EXAFS curve-fitting results (broken lines) to the spectra (solid lines).

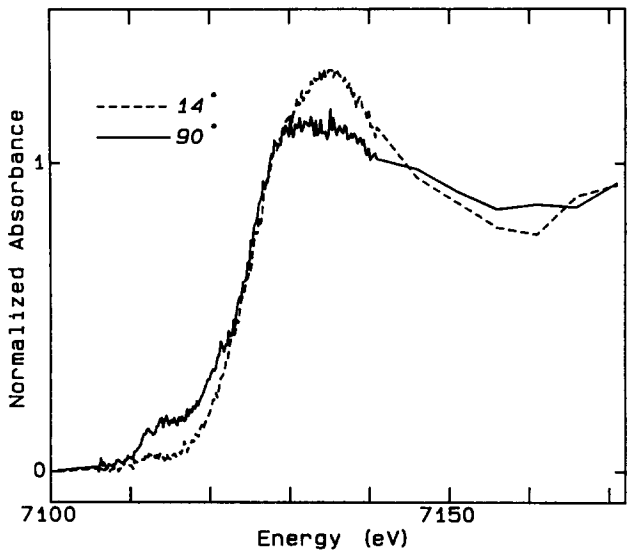

Fig. 7. Iron K-edge spectra of oriented cytochrome oxidase.

is apparent, especially in the $1s \rightarrow 3d$ transition (which occurs at about 7113 eV) and in the peak at 7135 eV. The $1s \rightarrow 3d$ transition is quite pronounced when $\theta = 90°$ and is diminished at $\theta = 14°$, while for the 7135 eV feature the reverse is true. Compared to bivalent copper, there is very little single-crystal model compound X-ray absorption data for iron available in the literature and this makes interpretation difficult. Single crystal spectra of heme model compounds [45] do, however, indicate that our results are fully consistent with the heme orientation perpendicular to the membrane found in earlier work [6–9].

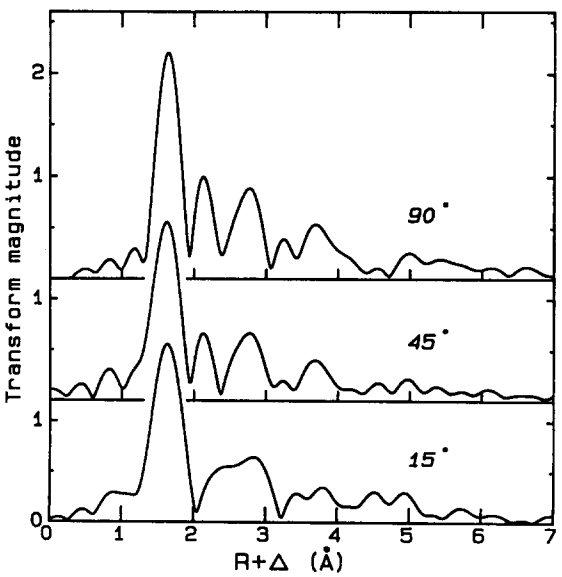

Fig. 8. Iron K-edge EXAFS Fourier transforms of oriented cytochrome oxidase.

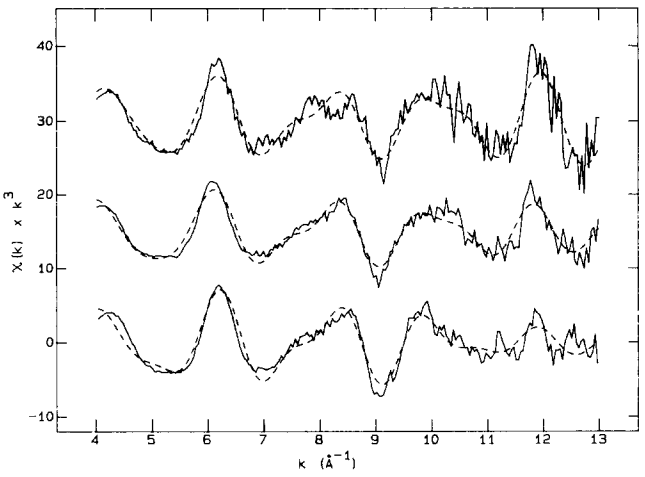

Fig. 9. Iron K-edge EXAFS spectra (solid lines) and best fits (broken lines) of oriented cytochrome oxidase. The fits illustrated were calculated using the parameters given in Table II.

Iron EXAFS Fourier transforms and EXAFS curve fitting

Previous work, using EPR and optical spectroscopies, has shown that both the hemes are oriented perpendicular to the membrane [6–9]. The iron EXAFS at $\theta \rightarrow 0°$ is therefore expected to sense primarily iron-porphyrin contributions, while data taken at $\theta = 90°$ are expected to show axial ligand contributions. Heme *a* is thought to possess two axial histidine ligands [46], while heme a_3 is thought to possess one axial histidine, plus the bridging ligand to Cu_B [46]. The iron EXAFS Fourier transforms are shown in Fig. 8. All orientations show the expected first shell Fe–N interaction and outer-shell Fe–C interactions from the histidine and porphyrin carbons. An additional peak at $R + \Delta = 2.1$ Å, which is most intense in the 90° data, indicates the presence of an axial Fe-(S/Cl) type of ligand to one of the irons. Similar features have been observed in cytochrome oxidase iron EXAFS Fourier transforms by Powers, Chance and co-workers [11–13]. EXAFS curve fitting (Fig. 9, Table II) requires the presence of at least two different Fe-N distances for the 15° data ($R = 2.05$ and 1.95 Å), which is consistent with the presence of one high spin ($R = 2.05$ Å) and

TABLE II

Curve-fitting parameters for cytochrome oxidase oriented membranous multilayer iron EXAFS

The values for σ^2 were fixed at the chemically reasonable value of 0.0025 Å^2, which was also the all-round best-fit value.

	$Fe-N_a$		$Fe-N_b$		Fe–S	
θ	$F(\theta)\,N$	R (Å)	$F(\theta)\,N$	R (Å)	$F(\theta)\,N$	R (Å)
15°	4.70	2.045	2.30	1.950	0.00	–
45°	4.22	2.025	1.20	2.013	0.40	2.357
90°	3.50	2.010	0.00	–	1.51	2.317

TABLE III

Curve-fitting parameters for cytochrome oxidase oriented membranous multilayer zinc EXAFS

The values for σ^2 were fixed at the chemically reasonable value of 0.0025 Å^2, which was also the all-round best-fit value.

	Zn–N		Zn–S	
θ	$F(\theta)\,N$	R (Å)	$F(\theta)\,N$	R (Å)
15°	0.937	2.116	3.104	2.332
90°	0.00	–	3.114	2.336

one low spin ($R = 1.95$ Å) heme. At $\theta = 90°$ only one Fe-N distance was required, reflecting the smaller contribution of the equatorial nitrogens and the increased contribution of axial histidine nitrogens. For the data taken at $\theta = 90°$ and 45° an additional Fe–(S/Cl) interaction with $R = 2.33$ Å was required for an adequate fit. This interaction is similar to that reported earlier by Powers, Chance and co-workers [11–13], although a rather longer bond length of 2.6 Å was obtained by these workers. It may originate from a bridging ligand between heme a_3 and Cu_B. The results of the curve fitting analysis are summarized in Table II.

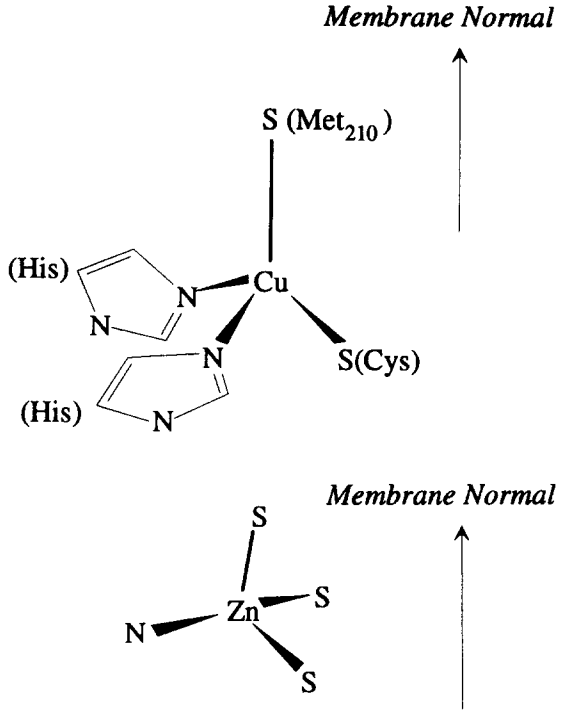

Fig. 11. Possible structures of the Cu_A and zinc metal sites in cytochrome oxidase, based on spectroscopic data, in combination with protein sequence data.

Zinc EXAFS Fourier transforms and EXAFS curve fitting

The zinc EXAFS of cytochrome oxidase has been previously investigated by two different groups and, despite some small differences in bond lengths, both conclude that zinc is coordinated by three sulfur or chlorine ligands and a single oxygen or nitrogen [17,47]. The zinc EXAFS Fourier transforms of membranous cytochrome oxidase at two different orientations are shown in Fig. 10a and the EXAFS spectra, together with the curve-fitting results in Fig. 10b. The pronounced Fourier transform peak close to $R + \Delta = 2.0$ Å is attributable to the Zn–(S,Cl) interactions and the smaller peak at $R + \Delta = 1.4$ Å to Zn–(O,N) interactions. While the Zn–(S,Cl) shows little angular dependence, the Zn–(O,N) interaction is detected only when

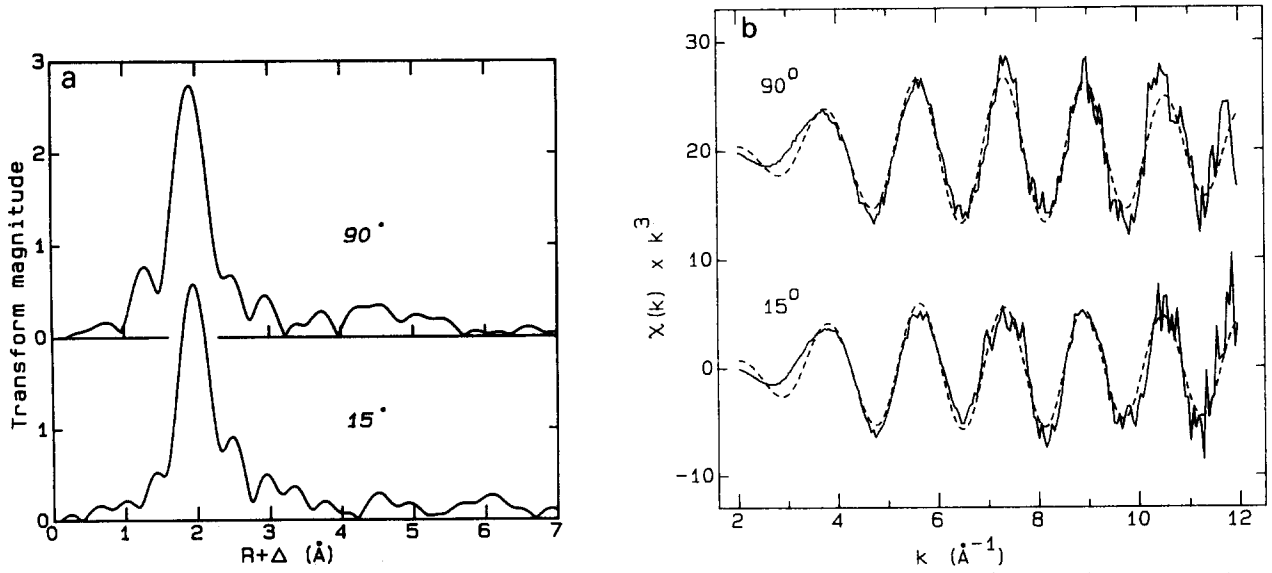

Fig. 10. (a) Zinc K-edge EXAFS Fourier transforms of oriented cytochrome oxidase. (b) Zinc EXAFS spectra (solid lines) and best fits (broken lines) using the parameters in Table III.

$\theta = 90°$. We conclude that the Zn-(O,N) bond is oriented with $\phi \cong 90°$, i.e. approximately in the membrane plane, while the Zn-(S,Cl) bonds have $\langle\phi\rangle \cong 50°$. This is consistent with a C_{3v} type site symmetry, i.e., an approximately tetrahedral coordination, which is a common geometry for zinc, with the Zn-(O,N) bond in the membrane plane (Fig. 11.

Discussion

Coordination of the Cu_A site

Amino acid sequence data are available for cytochrome oxidases from many different organisms and they show remarkable conservation. For example, the enzymes from the archaebacteria *Halobacterium halobium* [48] and *Sulfolobus acidocalderius* [49] are recognisably similar to those of eubacteria and eukaryotes [50–52], suggesting that conclusions about potential physiology based on taxonomic position should be drawn with caution. Comparisons of conserved regions have been useful in identifying probable metal sites [46,48–52]. Most eukaryotic cytochrome oxidases have three mitochondrially coded major subunits, called I, II and III. All four redox metals appear to reside in the two largest subunits; I and II. Subunit I is thought to bind heme *a* and the Cu_B-heme a_3 binuclear site, while subunit II is supposed to contain Cu_A. The probable site of Cu_A binding in subunit II is a short, highly conserved, region of the polypeptide chain which resembles the copper binding site of the type 1 copper proteins. Indeed, it was the existence of this partial homology which led to the identification of subunit II as the probable site for Cu_A, which was consistent with the long-held view that Cu_A is ligated by two cysteine and two histidine ligands. It is now well established that Cu_A is certainly not a type 1 copper site, and it is possible that the true binding site has yet to be identified. There is strong evidence from ENDOR spectroscopy that at least one histidine and at least one cysteine residue coordinate Cu_A [39,53]. There are doubts, however, as to the number of cysteine ligands to Cu_A. Zimmermann et al. [54] have described an alternate terminal oxidase from *Thermus thermophilus*. This enzyme contains heme *b* (instead of heme *a*?), a heme a_3-Cu_B binuclear site and Cu_A (as identified by EPR spectroscopy), bound to a single polypeptide of about 35 000 molecular weight. Amino-acid analysis of the enzyme indicated the presence of about eight methionines, eight or nine histidines but only a single cysteine residue [54]. Thus, as pointed out by Zimmermann et al. [54], if this enzyme does indeed contain Cu_A, and if the analysis is correct, the traditional model for the Cu_A binding site must be in error.

The 2.6 Å Cu–(S,Cl) interaction could originate from a ligand of Cu_A or of Cu_B. Such a bond length is rather too long for a typical thiolate ($R\text{-}S^-$) or chloride (Cl^-) ligand to copper. Two coordinations which would be expected to possess such a long bond length are 'bridging' thiolate or chloride, such as might connect Cu_B and heme a_3, and methionine ligands. The former possibility was favored in our preliminary report [41] because of comparisons with a model compound [55], but we now consider this possibility much less likely. Our finding of a 2.6 Å Cu–S interaction in cyanide-bound cytochrome oxidase (see above), in which the Cu_B-heme a_3 site is thought to be disrupted, makes the Cu_B-heme a_3 bridge seem a less probable site for this ligand. Additionally, if the 2.6 Å bond were a ligand of Cu_B, it would be expected to be axially coordinated to the tetragonal copper. The Cu K-edge spectra, as discussed above, suggest that the axial vector of Cu_B is oriented at 90° to the membrane normal, while the copper EXAFS indicates that the 2.6 Å Cu-(S,Cl) vector is oriented at 0°, and axial coordination would be impossible. The possiblility of a methionine ligand of Cu_A, oriented with the Cu-S vector along the membrane normal seems much more attractive. Subunit II contains a quite strongly conserved methionine residue (Met_{210} of the bovine enzyme), and the hypothesis that this is a ligand of Cu_A is consistent with recent magnetic circular dichroism results on oriented cytochrome oxidase [56], and with our speculation as to the nature of the Cu K-edge $1s \rightarrow 3d$ transition, discussed above. A role for methionine in coordinating Cu_A has also recently been proposed by Covello and Gray [57]. A possible structure for the Cu_A site is illustrated in Fig. 11.

Coordination of the Cu_B site

Assuming that the Cu_B site of the *T. thermophilus* oxidase is similar to conventional cytochrome oxidases, and assuming that the single cysteine is coordinated to Cu_A [54], the dearth of available sulfur coordination sites seems at odds with our estimate of 2–3 such ligands per copper. A possible explanation is that some of the putative sulfurs are in fact chloride ligands, and suggests a role for chloride as the bridging ligand for the binuclear site. This would be fully consistent with our data, and is supported by our preliminary results on the polarized iron EXAFS of the cyanide treated enzyme (data not shown), which lacks the iron EXAFS Fourier transform feature that we attribute to the 2.3 Å Fe-(S,Cl) bridging ligand (Fig. 8, Table II). A bridging role for chloride is also supported by recent results [17] which indicate that enzyme prepared in the absence of chloride lacks the 2.3 Å Fe-(S,Cl) iron EXAFS Fourier transform feature.

As the presumed site of oxygen reduction, the heme a_3-Cu_B binuclear site is perhaps the site of greatest interest in cytochrome oxidase, and knowledge of the separation of the metals is expected to be central in understanding the catalytic mechanism of the enzyme.

The problem of determining the structure of the Cu_B site in eukaryotic enzymes is exacerbated by the presence of Cu_A, as the copper EXAFS will always be a mixture of the spectra from both coppers. There are reports in the literature of EXAFS from enzyme depleted in Cu_A [58], but the rather harsh chemical treatment required to deplete Cu_A means that the results of this study must be treated with some skepticism. Perhaps X-ray spectroscopy of the recently discovered homologous enzyme from *Escherichia coli*, which lacks Cu_A [59–61], will shed additional light on this topic.

The distance between Cu_B and heme a_3 has been the subject of considerable debate in recent years. While Chance, Powers and co-workers [11] conclude that the Cu_B-Fe(a_3) separation is 3.8 Å, Scott and co-workers [16] deduce the rather smaller distance of 3.0 Å. According to Scott [17], the data from the two groups are essentially indistinguishable and, if this is indeed the case, then the cause of the disparate conclusions must have its root in different numerical analysis procedures. The presence of EXAFS from outer shell carbons of the iron porphyrin, and from histidine ligands to both iron and copper, will tend to confuse the assignment of any long-distance Cu–Fe interactions. This is especially true for copper, as the total phase-shift function, $\alpha(k)$, for Cu–Fe is displaced by close to 2π from that for Cu–C, making correct assignment rather difficult. For oriented samples, a Cu–Fe interaction must have the same angular dependence in both the copper and the iron EXAFS data, and thus ought to remove ambiguity in identifying this interaction. Moreover, the Cu–Fe interaction present in the resting enzyme ought to be altered in the cyanide-inhibited enzyme. The heme orientation, which is known to be perpendicular to the membrane, requires that the Cu-Fe vector cannot point along the membrane normal. The Cu-Fe bridging ligand is an axial ligand of iron, and assuming that the bond angle for the bridge is not very much less than 90°, then one would expect the Cu-Fe vector to be between 40° and 90° from the membrane normal. The former orientation would yield EXAFS with little dichroism, while the latter would have maximal EXAFS amplitude at $\theta = 90°$. Some long-distance features in the EXAFS do show significant anisotropy; for example the iron Fourier transform peak at $R + \Delta = 3.7$ Å is of maximum intensity at $\theta = 90°$ (Fig. 8); however, no corresponding dichroism is observed in the copper EXAFS (see Fig. 4).

The copper EXAFS Fourier transform feature assigned by Scott and co-workers as the Cu–Fe interaction is visible in our data (Fig. 4, Fig. 12) as a peak at R ≅ 3.0 Å, and this fits well to a Cu–Fe interaction at 3.01 Å (see Fig. 12). Unfortunately this distance coincides with the intense heme Fe–αC interaction, which prevents unambiguous support from the iron EXAFS. There is also significant dichroism in the supposed 3 Å Cu–Fe interaction, which would be consistent with a value for θ of about 60°–90° (not illustrated). We do not, however, consider the present data sufficient to make definitive conclusions concerning the Cu_B-Fe(a_3) separation. Some speculation, however, is perhaps in

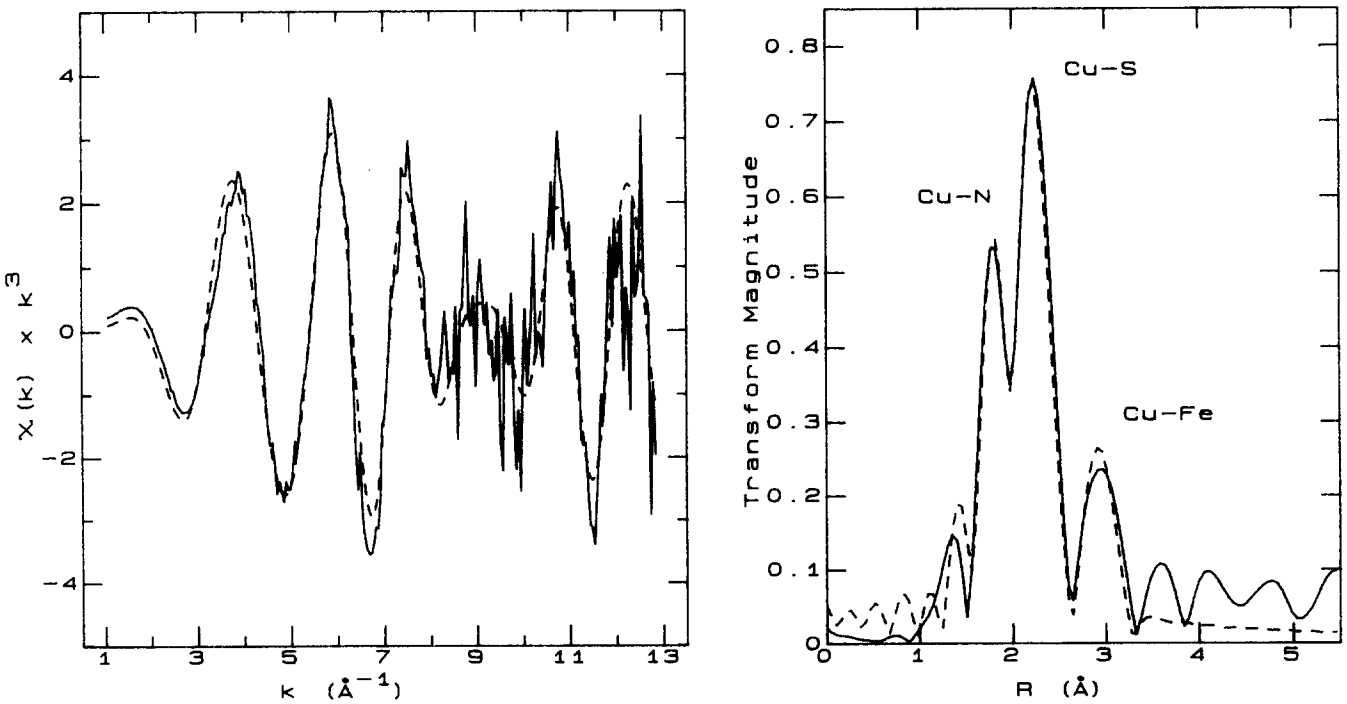

Fig. 12. Detail of curve-fitting results for the $\theta = 90°$ copper K-edge EXAFS (left panel) and EXAFS Fourier transforms (right panel). The broken lines show the best fit and the solid lines the experimental data.

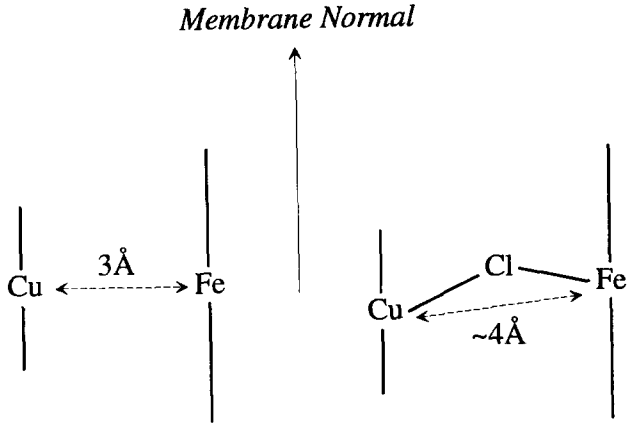

Fig. 13. Schematic diagram of possible structures for the Cu_B-Fe heme a_3 binuclear site.

order. The proposed copper-iron separation of 3.0 Å [16] seems rather too short to accomodate a bridging ligand between copper and iron, while the larger separation proposed by Powers, Chance and co-workers [11] of 3.8 Å leaves plenty of room for a bridging ligand such as chloride or sulfur. In view of the fact that cytochrome oxidase is known to exist in several different active forms [11–14,16,20–22,54], it seems quite plausable that the enzyme can exist in at least two different forms, with (4 Å Cu_B-Fe(a_3)), or without (3 Å Cu_B-Fe(a_3)) a bridging ligand (Fig. 13).

Acknowledgements

We are indebted to the Staff of the Stanford Synchrotron Radiation Laboratory (SSRL), for their assistance. SSRL is funded by the DOE (Office of Basic Energy Sciences, Division of Chemical Sciences) and NIH (Biotechnology Resource Program, Division of Research Resources).

References

1 Babcock, G.T. and Wikström, M.K.F. (1992) Nature 356, 301–309.
2 Han, S., Ching, Y-c. and Rousseau, D.L. (1990) Nature 348, 89–90.
3 Wikström, M. (1989) Nature 338, 776–778.
4 Yoshikawa, S., Tera, T., Takahashi, Y., Tsukihara, T. and Caughey, W. (1988) Proc. Natl. Acad. Sci. USA 85, 1354–1358.
5 Blasie, J.K., Erecinska, M., Samuels, S. and Leigh, J.S. (1978) Biochim. Biophys. Acta 501, 33–52.
6 Erecinska, M., Wilson, D.F. and Blasie, J.K. (1978) Biochim. Biophys. Acta 501, 53–62.
7 Erecinska, M., Wilson, D.F. and Blasie, J.K. (1978) Biochim. Biophys. Acta 501 63–71.
8 Erecinska, M., Wilson, D.F. and Blasie, J.K. (1978) Biochim. Biophys. Acta 545, 352–364.
9 Blum, H., Harmon, H.J., Leigh, J.S., Salerno, J.C. and Chance, B. (1978) Biochim. Biophys. Acta 502, 1–10.
10 Onishi, T., LoBrutto, R., Salerno, J.C., Bruckner, R.C. and Frey, T.G. (1982) J. Biol. Chem. 257, 14821–14825.
11 Powers, L., Blumberg, W., Chance, B., Barlow, C., Leigh, J.S., Smith, J., Yonetani, T., Vik, S. and Peisach J. (1979) Biochim. Biophys. Acta 546, 520–531.
12 Powers, L. and Chance, B. (1984) in EXAFS and Near-Edge Structure III (Hodgson K.O., Hedman, B. and Penner-Hahn, J.E., eds.), pp. 117–123, Springer-Verlag, Berlin.
13 Powers, L. and Chance, B. (1985) Inorg. Biochem. 23, 207–217.
14 Scott, R.A., Schwartz, J.R. and Cramer, S.P. (1984) in EXAFS and Near-Edge Structure III (Hodgson K.O., Hedman, B. and Penner-Hahn, J.E., eds.), pp. 111–116, Springer-Verlag, Berlin.
15 Scott, R.A., Schwartz, J.R. and Cramer, S.P. (1985) in Biological & Inorganic Copper Chemistry (Karlin, K.D. and Zubieta, J., eds.), pp. 41–52, Adenine Press.
16 Scott, R.A., Schwartz, J.R. and Cramer, S.P. (1986) Biochemistry 25, 5546–5455.
17 Scott, R.A. (1989) Annu. Rev. Biophys. Biophys. Chem. 18, 137–158.
18 Frey, T.G., Chan, S.H.P. and Schatz, G. (1978) J. Biol. Chem. 253, 4389–4395.
19 Brudvig, G.W., Stevens, T.H., Morse, R.H. and Chan, S.I. (1981) Biochemistry 20, 3912–3921.
20 Naqui, A., Kumar, C., Ching, Y., Powers, L. and Chance, B. (1984) Biochemistry 23, 6222–6227.
21 Baker, G.W., Noguchi, M., Palmer, G. (1987) Biochemistry 262, 595–604.
22 Moody, A.J., Cooper, C.E. and Rich, P.R. (1991) Biochim. Biophys. Acta 1059, 189–207.
23 Cramer, S.P. and Scott, R.A. (1981) Rev. Sci. Instrum. 52, 395–399.
24 Stern, E.A. and Heald, S.M., (1979) Rev. Sci. Instrum. 50, 1579–1582.
25 Cramer, S.P., Tench, O., Yocum, M. and George, G.N. (1988) Nucl. Instr. Methods A266, 586–591.
26 Rehr, J.J., Mustre de Leon, J., Zabinsky, S.I. and Albers, R.C. (1991) J. Am. Chem. Soc. 113, 5135–5140.
27 Mustre de Leon, J., Rehr, J.J. and Zabinsky, S.I. (1991) Phys. Rev. B, 44, 4146–4156.
28 Brouder, C. (1990) J. Phys.: Condens. Matter 2, 701–738.
29 George, G.N., Prince, R.C. and Cramer, S.P. (1989) Science 243, 789–791.
30 George, G.N., Prince, R.C., Frey, T.G. and Cramer, S.P. (1989) Physica B 158, 81–83.
31 McMaster, W.H., Kerr Del Grande, N., Mallet, J.H. and Hubbel, J.H. (1965) Compelation of X-ray Cross-Sections. (Natl. Bureau of Standards).
32 Palmer, G. (1987) Pure Appl. Chem. 59, 749–758.
33 Steffens, G.C.M., Biewald, R. and Buse, G. (1987) Eur. J. Biochem. 164, 295–300
34 Kroneck, P.M.H., Antholine, W.A., Riester, J. and Zumft, W.G. (1988) FEBS Lett. 242, 70–74.
35 Hahn, J.E., Scott, R.A., Hodgson, K.O., Doniach, S., Desjardins, S.R. and Solomon, E.I. (1982) Chem. Phys. Lett. 88, 595–598.
36 Kosugi, N., Yokoyama, K., Asakura, K. and Kuroda, H. (1984) Chem. Phys. 91, 249–256.
37 Smith, T.A., Penner-Hahn, J.E., Berding, M.A., Doniach, S. and Hodgson, K.O. (1985) J. Am. Chem. Soc. 107, 5945–5955.
38 Yokoyama, K., Kosugi, N. and Kuroda, H. (1986) Chem. Phys. 103, 101–109.
39 Martin, C.T., Scholes, C.P. and Chan, S.I. (1988) J. Biol. Chem. 263, 8420–8429.
40 Penner-Hahn, J.E., Murata, M., Hodgson, K.O. and Freeman, H. (1989) Inorg. Chem. 28, 1826–1832.
41 George, G.N., Prince, R.C., Frey, T.G. and Cramer, S.P. (1988) Adv. Memb. Biochem. Bioenerg. (Kim, C.H., et al., Eds.) pp. 429–438, Plenum Press.
42 Scott, R.A., Zumft, W.G., Coyle, C.L. and Dooley, D.M. (1989) Proc. NAtl. Acad. Sci. USA 86, 4082–4086.

43 Yoshikawa, S. and Winslow, S.C. (1990) J. Biol. Chem. 265, 7945–7958.
44 Scott, R.A., Schwartz, J.R. and Cramer, S.P. (1985) J. Inorg. Biochem. 23, 199–205.
45 Penner-Hahn, J.E., Wang, S. and Waldo, G.S. (1991) in X-ray Absorption Fine Structure (Hasnain, S., Ed.), pp 147–151.
46 Holm, L., Saraste, M. and Wikström, M. (1987) EMBO J. 6, 2819–2823.
47 Naqui, A., Powers, L., Lundeen, M., Cinstantinescu, A. and Chance, B. (1988) J. Biol. Chem. 263, 12342–12345.
48 Denda, K., Taketomo, F., Makoto, S., Masasuke, Y., Fukumori, Y. and Yamanaka, T. (1991) Biochem. Biophys. Res. Commun. 181, 316–322.
49 Luebben, M., Kolmerer, B. and Saraste, M. (1992) EMBO J. 11, 805–812.
50 Malmström, B.G. (1990) Chem. Rev. 90, 1247–1260.
51 Saraste, M. (1990) Quart. Rev. Biophys. 23, 331–366.
52 Capaldi, R.A. (1990) Annu. Rev. Biochem. 59, 569–596.
53 Stevens, T.H., Martin, C.T., Wang, H., Brudvig, G.W., Scholes, C.P. and Chan, S.I. (1982) J. Biol. Chem. 257, 12106–12113.
54 Zimmermann, B.H., Nitschi, C.I., Fee, J.A., Rusnak, F. and Münk, E. (1988) Proc. Natl. Acad. Sci. USA 85, 5779–5783.
55 Schauer, C.K., Akabori, K., Elliot, C.M. and Anderson, O.P. (1984) J. Am. Chem. Soc. 106, 1128–1130.
56 Thomson, A.J., Greenwood, C., Peterson, J. and Barrett C.P. (1986) J. Inorg. Biochem. 195–205.
57 Covello, P.S. and Gray, M.W. (1990) FEBS Lett. 268, 5–7.
58 Li, P.M., Gelles, J., Chan, S.I., Sullivan, R.J. and Scott, R.A. (1987) Biochemistry 26, 2091–2095.
59 Chepuri, V., Lemieux, L., Au, D.C.T. and Gennis, R.B. (1990) J. Biol. Chem. 265, 11185–11192.
60 Lauraeus, M., Maltia, T., Saraste, M. and Wikström, M.F.K.(1991) Eur. J. Biochem. 197, 699–705.
61 Puustinen, A., Finel, M., Haltia, T. and Gennis, R.B. (1991) Biochemistry 30, 3936–3942.